Available online at www.sciencedirect.com

SciVerse ScienceDirect

Ceramics International 39 (2013) 4481–4488

CERAMICS INTERNATIONAL

www.elsevier.com/locate/ceramint

Influence of ethanol supercritical drying treatment on morphology and electrochemical properties of $DyBaCo_2O_{5+\delta}$ cathode material

Ming-Wen Xiong, Xianxia Yuan, Jie-Wei Yin, Yi-Mei Yin, Zi-Feng Ma*

School of Chemistry and Chemical Engineering, Shanghai Jiao Tong University, Shanghai 200240, PR China

Received 4 October 2012; received in revised form 15 November 2012; accepted 16 November 2012
Available online 28 November 2012

Abstract

Effects of ethanol supercritical drying treatment on morphology and electrochemical performance of $DyBaCo_2O_{5+\delta}$ (DBC), as cathode material for intermediate temperature solid oxide fuel cells (IT-SOFCs), was comparatively investigated. Powder samples were synthesized by EDTA–citric acid (EC) and ethanol supercritical drying assisted EDTA–citric acid (SCEC) techniques. The scanning electron microscopy (SEM) images show the particles synthesized by SCEC were smaller than those prepared by the EC method. The area specific resistance (ASR) value of SCEC-DBC as cathode was lower than that of DBC-EC cathode. The maximum power density of the single cell with SCEC-DBC cathode was higher than that of the cell with EC-DBC cathode in the investigated temperature range from 550 to 650 °C.

Keywords: A. Ethanol supercritical drying treatment; B. Morphology; C. Polarization resistance; E. Cathode material

1. Introduction

Cathode polarization resistance is a major source of the total resistance in solid oxide fuel cells (SOFC) and becomes even more significant as the operating temperatures are reduced to intermediate range (500–700 °C) [1–3]. To overcome this drawback, the development of advanced cathode materials and optimization of cathode microstructures are therefore critical to intermediate temperature solid oxide fuel cells (IT-SOFC) [4,5]. The previous investigations demonstrated that synthesis methods and powder processing conditions significantly influence the morphology and crystallite dimension of the resulting powders, so as to the cathode performance. To obtain materials with good properties, many different powder synthesis techniques, such as solid–state reaction, combustion, co-precipitation, microwave synthesis, spray pyrolysis and sol–gel technique, have been employed [6–11]. Although the common sol–gel technique is a particularly useful one among the above mentioned methods in producing superfine ceramic powders, the combustion of the large amount organic component still easily leads to agglomeration of small particles. How to easily remove the organic residue in the gel and avoid destroying the distribution of the metal ions becomes a considerable issue. Supercritical fluids assisted drying technique is widely accepted to produce nano-materials, which allows removing most organic precursors in gels since its drying process is under zero surface tension condition, therefore avoiding agglomeration of metal ions [12]. To the best of our knowledge, the study of effect of supercritical drying treatment on morphology and electrochemical properties of starting powder as cathode for IT-SOFCs is still scanty. For obtaining homogeneous and highly reactive ceramic powders with small average particle size and high porosity, ethanol supercritical drying assisted sol–gel technique is a novel and expectable route to produce the promising IT-SOFCs cathode materials. Recently, layered cobalt-based oxides $LnBaCo_2O_{5+\delta}$ (Ln = Lanthanide elements) with double perovskite-type lattice structure exhibit excellent electronic and oxygen ionic conductivity properties, which are beneficial for the cathodes of IT-SOFCs [13–22]. Kim and Manthiram systematically investigated the influence of different Ln^{3+} ions on the structure, thermal expansion

*Corresponding author. Tel.: +86 21 54742894; fax: +86 21 54747717.
E-mail address: zfma@sjtu.edu.cn (Z.-F. Ma).

0272-8842/$ - see front matter © 2012 Elsevier Ltd and Techna Group S.r.l. All rights reserved.
http://dx.doi.org/10.1016/j.ceramint.2012.11.042

coefficient (TEC) and electrochemical properties of $LnBaCo_2O_{5+\delta}$ oxides, the results showed that the $LnBaCo_2O_{5+\delta}$ cathodes with an intermediate-size lanthanide ion, such as Nd^{3+}, Sm^{3+} and Dy^{3+}, might provide a trade-off between TEC and catalytic activity [23]. In the present research, we synthesized $DyBaCo_2O_{5+\delta}$ via EDTA–citric acid (EC) and ethanol supercritical drying assisted EDTA–citric acid (SCEC) methods, and the effects of supercritical fluids assisted drying on microstructure and electrochemical performance of as-prepared cathodes were comparatively investigated and analyzed.

2. Experimental

2.1. Material synthesis

$DyBaCo_2O_{5+\delta}$ (DBC) powders were prepared by the EC and SCEC methods. Appropriate amounts of metal nitrates were dissolved in EDTA–ammonia solution (pH = 6–7) followed by the addition of citric acid, wherein the molar ratio of total metal ions: EDTA: citric acid is 1:1:2 and the EDTA and citric acid acts as complexing agents. Then, the brown solution was gelated at 80 °C with constant stirring and ammonia was used to ensure the pH value of around 7. For the EC method, the gel was transferred to an oven and heat-treated at 260 °C for 2 h to obtain a primary powder, which was subsequently calcined at 950 °C for 2 h under an air atmosphere to obtain the well-crystallized powders (named as EC-DBC). For the SCEC method, the gel was transferred into an autoclave, followed by raising temperature to 220 °C and keeping for half an hour. Then, the supercritical fluid drying process was operated at 260 °C for 2 h under a pressure of 8 M Pa. After slowly releasing the vapor inside, the system was allowed to cool down to room temperature. Ultimately, the as-prepared powders were calcined at 950 °C in air for 2 h to obtain the final powder (named as SCEC-DBC).

2.2. Characterization

Thermogravimetric analysis (TG) and differential thermal analysis (DTA) of the as-prepared powders were performed on a thermal analyzer instrument (DTG-60, Shimadzu) with a heating rate of 10 °C min^{-1} in flowing air. The morphology and sizes of the DBC powders were examined using scanning electron microscopy equipped with energy dispersive X-ray (EDX) spectroscopy (S-4800, Hitachi).

2.3. Cell fabrication and electrochemical performance measurement

A symmetrical cell with the configuration of DBC|SDC|DBC was used for the impedance studies. Firstly, SDC powders were pressed into a pellet and sintered at 1450 °C for 5 h in air to obtain a SDC pellet with 12 mm in diameter and 0.5 mm in thickness. To prepare the electrode, the DBC oxide powders were dispersed in a premixed solution of glycerol, ethylene glycol and isopropyl alcohol to form a suspension by high-energy ball milling (Pulverisettle 6, Fritsch) at the rotation rate of 400 rpm for 2 h. The obtained DBC slurry was sprayed symmetrically on both surfaces of the SDC pellet, followed by calcined at 1000 °C for 5 h under stagnant air. The silver paste was then applied to both electrode surfaces to act as the current collector. The area of the used cathode was 0.55 cm^2. Anode-supported cells with $Sm_{0.2}Ce_{0.8}O_{1.9}$ (SDC) as electrolyte were prepared by a co-pressing technique. Anode powders consisted of 65% NiO and 35% SDC (in weight) were prepared by mixing NiO and SDC in an agate mortar. The well mixed NiO–SDC powder was firstly pressed into pellets with a diameter of 13 mm as a substrate, SDC powder was then added onto the substrate and co-pressed to form a green bi-layer pellet. The bi-layer pellet was subsequently sintered at 1400 °C for the densification of the electrolyte layer. The DBC-based slurry was sprayed onto the central surface of the electrolyte and sintered at 1000 °C for 2 h under air atmosphere. The effective area of the resulted cathode is about 0.26 cm^2 and the layer thickness of electrolyte is around 20 μm. Electrochemical impedances of the symmetrical cells were characterized by a potentiostat/galvanostat of IM6 from Zahner Corporation (German) in a frequency range from 10 kHz to 0.5 Hz with an AC amplitude of 10 mV and in the temperature range from 550 °C to 700 °C at 50 °C intervals. The performance of the obtained cells were collected by a source meter (2420, Keithley).

3. Results and discussion

Fig. 1 presents TGA and DTA curves of the DBC precursors synthesized by the EC and SCEC methods before calcination. The weight losses in the temperature range from 30 °C to 200 °C can be ascribed to the desorption of physically absorbed water and trapped ammonia accompanied by small endothermic peaks at around 100 °C. After that, drastic weight losses are observed in the TGA curves in the temperature range from 200 °C to 700 °C and 200 °C to 500 °C for the SECE-DBC and EC-DBC, respectively. The accompanied exothermic peaks in DTA curves indicate multiple steps responsible for the decomposition and combustion of metal-complexes agents and nitrates and crystallization of DBC oxides. The combustion of organic complexes after decomposition process delivers large amount of heat which is the main cause for observed weight losses in TG curves and sharp heat in DTA curves. Therefore, almost all of the organic complexing components remained in the sample prepared by EC method, leading to a broad and strong exothermic peak in DTA cure. However, a large portion of the complexing agents in the SCEC-DBC sample have been dissolved in the supercritical ethanol and removed along with ethanol vapor during the deaerating process, leading to the exothermic peaks at 443 °C and 645 °C. The former peak at 443 °C corresponds to the

combustion of organic constituents, and the later one is to crystallization of DBC oxides. The small weight loss at temperature higher than 700 °C and 500 °C for the SECE-DBC and EC-DBC, respectively, is due to the removal of oxygen from the lattice, indicating that the decomposition and combustion of the complexing agents has completed. In addition, the much lower weight loss of SECE-DBC than that of EC-DBC suggests that ethanol supercritical drying treatment is helpful to the removal of organic complexing agents [12,24–27].

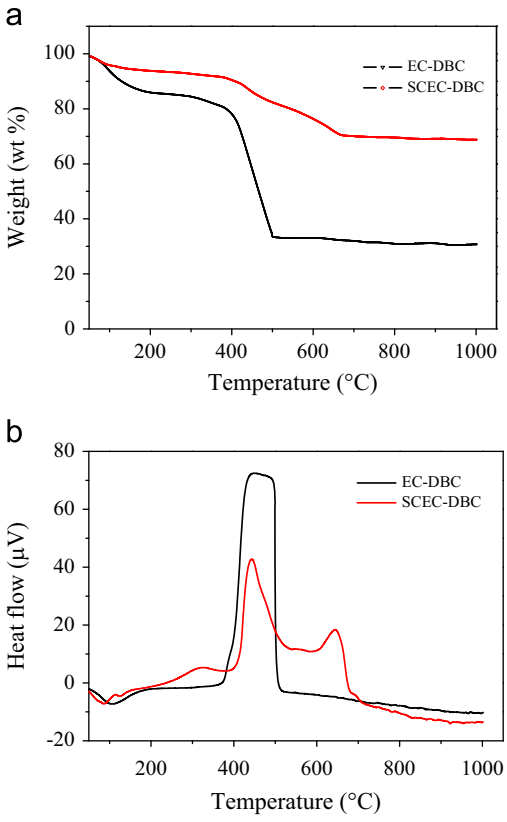

Fig. 1. TGA (a) and DTA (b) curves for the DBC precursors prepared by the EC and SCEC methods.

Fig. 2 shows the SEM images of DBC powders synthesized by the EC and SCEC methods. It can be noted that the powders synthesized via the EC method have spherical shape with the particle size varying from 0.5 to 1 μm whereas the powders obtained by the SCEC method have sponge-like shape consisted of small-size and uniform particles. The EC-DBC powders with large particle size are due to agglomeration of the metal ions needed for the oxide, which is caused by delivered heat from the combustion of the organic residues. On the other hand, the particle size is also affected by the calcinating temperature. The combustion of the large amount of organic residual in EC-DBC powders leads to high temperature in some areas leading to agglomeration of the small size particles. In addition, the different morphology of the two samples demonstrates that ethanol supercritical drying treatment plays a crucial role in preparation process of the DBC Powders. Supercritical ethanol fluid with little surface tension can diffuse into the DBC gel to form a mixture of ethanol and organic complexing agents, while the mixture with no tension can be easily removed from the nano-sized network, thus the stable and porous network structure remains without destroy in SCEC-DBC sample [28].

Fig. 3 presents the elemental mapping of the DBC powders obtained by the EC and SCEC methods. The distributions of Dy, Ba, Co and O in most of EC-DBC powders (Fig. 3a) and SCEC-DBC powders (Fig. 3c) are homogenous. However, agglomeration of the metal ions is also observed in Fig. 3(b) for the EC-DBC powders. Therefore, it could be figured out that the distributions of Dy, Ba, Co and O in SCEC-DBC powders are more homogeneous than those in DBC-SC powders.

The area specific resistance (ASR) is an important index used to evaluate the performance of cathode, which can be obtained from the Nyquist plots of the electrochemical impedance spectra (EIS). Therefore, the cathode performance for DBC was investigated by EIS based on a symmetrical cell with a configuration of DBC|SDC|DBC. Fig. 4 shows the obtained Nyquist plots measured at open

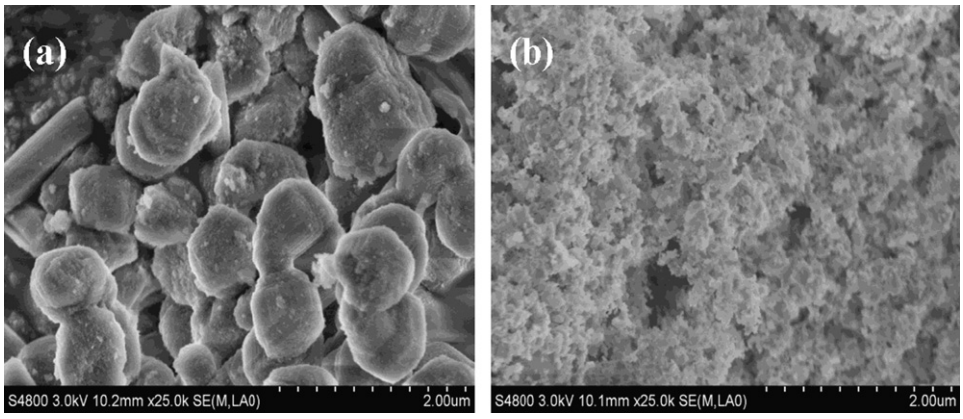

Fig. 2. SEM of DBC powders prepared with different methods: (a) EC and (b) SCEC.

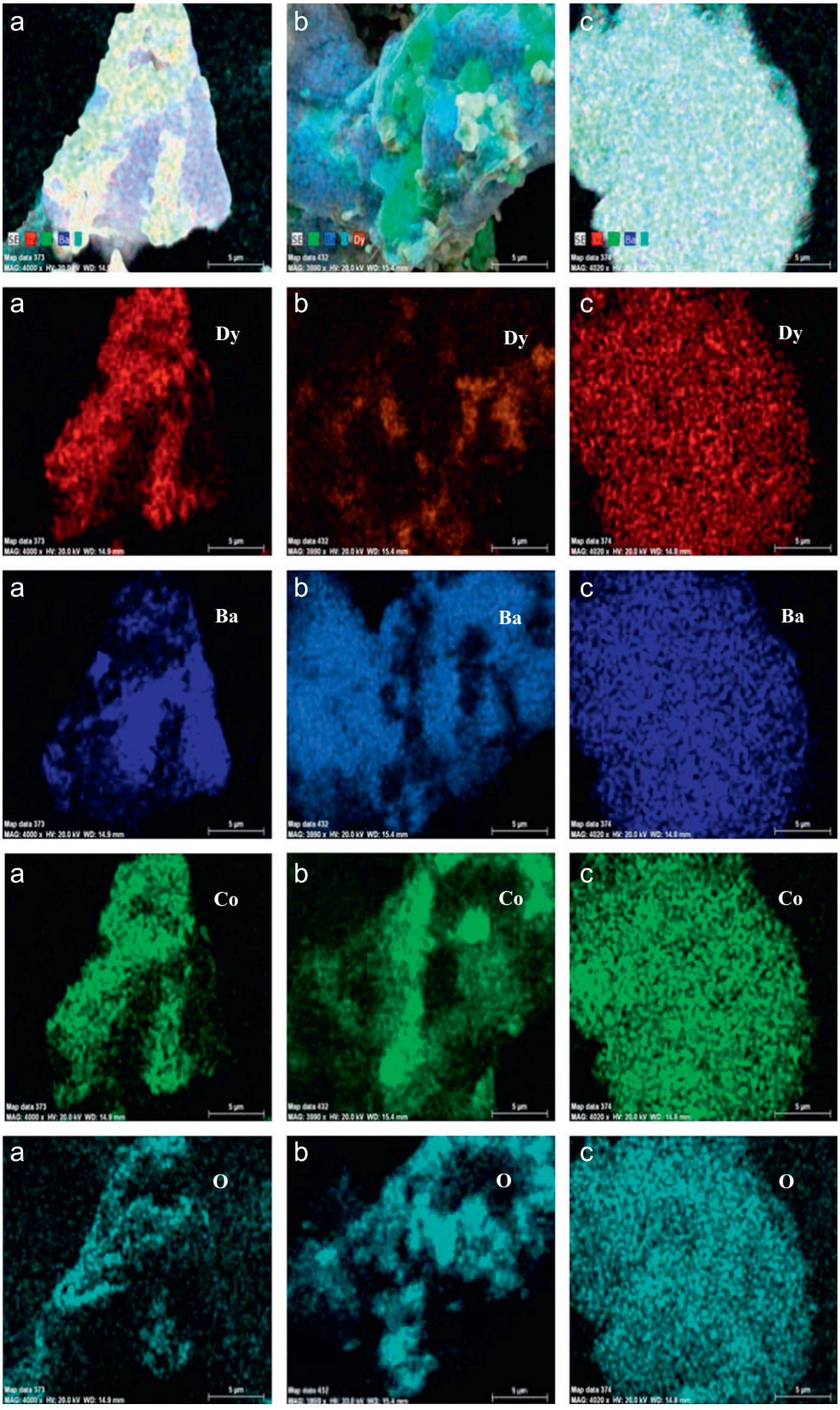

Fig. 3. EDS elemental mapping showing the distribution of Dy, Ba, Co and O elements in powders prepared with different methods: (a) most of EC, (b) agglomeration in EC and (c) SCEC.

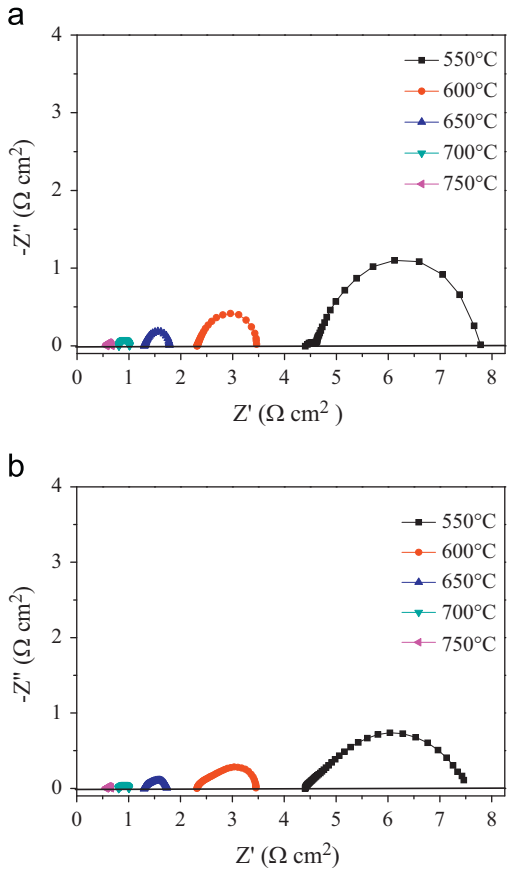

Fig. 4. Typical electrochemical impedance spectra of EC-DBC|SDC|EC-DBC and SCEC-DBC|SDC|SCEC-DBC symmetric cells measured at various temperatures under open-circuit condition. (a) DBC-EC and (b) DBC-SCEC.

Table 1
ASR data for EC-DBC and SCEC-DBC cathodes on SDC electrolyte measured at different temperatures in air.

Temperature (°C)	550	600	650	700	750
EC-DBC (Ω cm^2)	3.968	1.374	0.493	0.223	0.101
SCEC-DBC (Ω cm^2)	3.053	1.132	0.435	0.197	0.096

circuit in the temperature range of 550–750 °C, in air, for the samples prepared by the EC and SCEC methods. The high frequency intercept with the real axis represents the total ohmic resistance of the symmetrical cell, including the resistance of the electrolyte, the two electrodes, the current collectors and the lead wires. The low frequency intercept corresponds to the overall resistance of the cell, and the difference between the two intercept values is attributed to the cathode polarization area specific resistance of DBC electrodes resulted from charge-transfer resistance, oxygen adsorption/desorption on the electrode surface and the diffusion of oxygen ions resistance [29–33]. As expected, The ASR decreases significantly with increase in temperature for both electrodes. The evolution of the ASR for EC-DBC and SCEC-DBC electrodes with temperature is given in Table 1. SCEC-DBC electrode shows lower ASR at each temperature compared to the EC-DBC cathode, and the

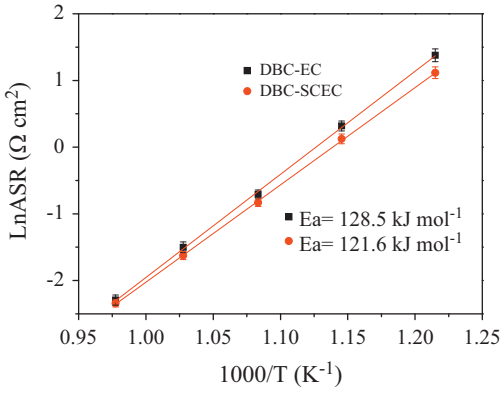

Fig. 5. Arrhenius plots of ASRs for cathode of EC-DBC and SCEC-DBC.

difference becomes more and more noticeable with the decrease of temperature. The induced Arrhenius plots are shown in Fig. 5 and the calculated value of apparent activation energy for SCEC-DBC is 121.6 kJ mol^{-1} compared to that of 128.5 kJ mol^{-1} for EC-DBC. The difference in ASR and apparent activation energy for EC-DBC and SCEC-DBC cathodes can be ascribed to the microstructure change of electrode layer and the interface between electrode and electrolyte.

Fig. 6 shows the cross-sectional microstructures at the electrode/electrolyte of the fractured symmetrical cells after electrochemical test. It can be noted that the SDC electrolyte was fully dense and both cathode layers were porous and well adhered to the electrolyte surface. Besides, the way of particle stacking and the distribution of porosity in cathode layers were different. The EC-DBC cathode layer was fabricated with large DBC particles whereas the SCEC-DBC one was composed of small and uniform particles, leading to larger specific surface than in the former, which is beneficial to contacting of catalyst surface and oxygen.

To further interpret the effect of particle morphology on the electrochemical performance, the schematic diagrams of interface model of a symmetrical cell is shown in Fig. 7. Due to the porosity of the electrode, the contact regions between electrode and electrolyte consist of many intermittent contact points rather than fully continuous areas. Based on the assumption that the contact point is round plane and the areas of all the contact points are equal to each other under the same sintering conditions in the interface model, the contact areas are closely relative to the number of contact points at electrode/electrolyte interface, while this number could be mainly affected by the particle size in electrode. Therefore, the electrode made up of small particles possesses more contact points and higher contact areas, which provides multiple pathways for electron and oxygen ions transfer between electrode and electrolyte, and leads to the reduction in contact resistance [34]. Moreover, the smaller particles can easily form more porous channels in cathode layer that are beneficial for oxygen diffusion to the inner surface of cathode leading to reduced gas diffusion resistance. In addition, small

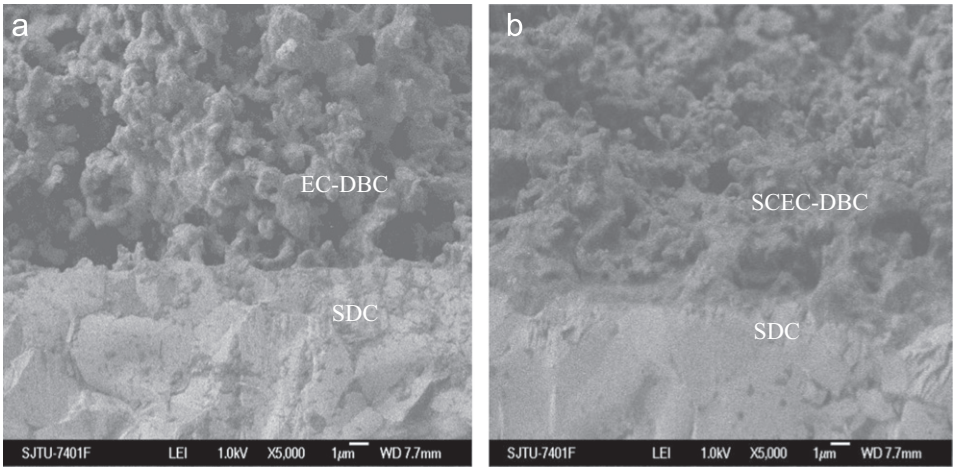

Fig. 6. SEM images of the cross-sectional microstructures after electrochemical testing: (a) EC-DBC and (b) SCEC-DBC.

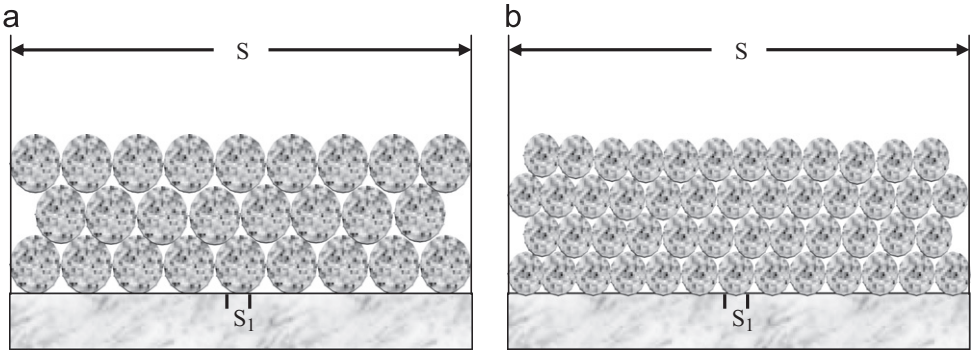

Fig. 7. Schematic diagrams of the interface model of a symmetrical cell.

particles could increase the gas–solid interface area in electrode for oxygen adsorption and dissociation, thus provide more active reaction sites of oxygen reduction reaction on the cathode surface and promote the oxygen ions transfer process from surface to bulk of cathode, resulting in reduction of the resistance during the charge transfer process.

To examine the performance of EC-DBC cathode and EC-DBC cathode in real IT-SOFC, anode-supported cells consisting of Ni-SDC cermets anode, SDC electrolyte and the corresponding cathode were fabricated, and the cell performance at various operating temperatures are presented in Fig. 8. The power densities of both cells increase obviously with increase in the operating temperature, mainly because of the decreased electrolyte resistance and the improved catalytic activity of the cathode materials at higher temperatures. The cell with SCEC-DBC cathode exhibits an apparently higher power output than that obtained with an EC-DBC cathode in the studied temperature ranging from 550 to 650 °C. For example, the peak power density of the cell with SCEC-DBC cathode reaches 529.7 mW cm^{-2} at 650 °C, while it is 436.5 mW cm^{-2} for EC-DBC cathode. This implies that the cell with SCEC-DBC possesses better cathode performance than that with EC-DBC. Therefore, it could be figured out that ethanol supercritical drying treatment on DBC cathode material is beneficial to improve the electrochemical performance of the electrode for IT-SOFC.

4. Conclusion

The morphology and electrochemical characteristics of $DyBaCo_2O_{5+\delta}$ oxides synthesized by the EC and SCEC method have been investigated comparatively. The results indicate that ethanol supercritical drying treatment process has significant positive effect on morphology and the electrochemical performance of DBC powders. SCEC-derived DBC powders show smaller particle size and more porous morphology. EIS and the performance of single cells reveal that the cathode prepared from the SCEC-DBC powders has lower ASR than that from EC-DBC powders. The SCEC technology was proven to be a very attractive method applied to the synthesis of electrode powders for IT-SOFCs.

Acknowledgments

This work has been financially supported by the Natural Science Foundation of China (Nos. 21173147, 21176155), the

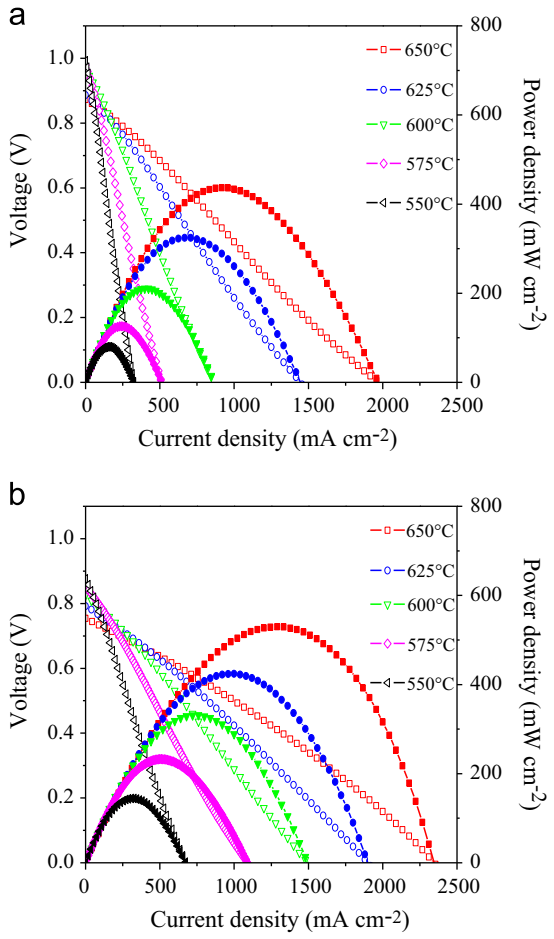

Fig. 8. Power density and voltage as a function of current density of the cell with (a) EC-DBC and (b) SCEC-DBC as cathode and NiO-SDC as anode with SDC electrolyte in the temperature range from 550 °C to 650 °C.

Science and Technology Commission of Shanghai Municipality (Nos. 10520708900, 10JC1406900). The authors are also thankful to Professor Zongping Shao at NJUT for his help with the cell performance test.

References

[1] Z. Shao, S.M. Haile, A high-performance cathode for the next generation of solid-oxide fuel, Nature 431 (2004) 170–173.

[2] K.K. Hansen, M. Søgaard, M. Mogensen, $Gd_{0.6}Sr_{0.4}Fe_{0.8}Co_{0.2}O_{3-\delta}$: a novel type of SOFC cathode, Electrochemical and Solid-State Letters 10 (2007) B119–B121.

[3] J.H. Kim, M. Cassidy, J.T.S. Irvine, J. Bae, Advanced electrochemical properties of $LnBa_{0.5}Sr_{0.5}Co_2O_{5+\delta}$ (Ln=Pr, Sm, and Gd) as cathode materials for IT-SOFC, Journal of the Electrochemical Society 156 (2009) B682–B689.

[4] K. Yashiro, T. Nakamura, M. Sase, F. Hermes, K. Sato, T. Kawada, J. Mizusaki, Composite cathode of perovskite-related oxides, $(La,Sr)CoO_{3-\delta}/(La,Sr)_2Co_{4-\delta}$, for solid oxide fuel cells, Electrochemical and Solid-State Letters 12 (2009) B135–B137.

[5] S.H. Chan, X.J. Chen, K.A. Khor, Cathode micromodel of solid oxide fuel cell, Journal of the Electrochemical Society 151 (2004) A164–A172.

[6] J. Zhang, H. Zhao, Y. Li, N. Xu, W. Ding, X. Lu, F. Li, Effects of iron content on the structural evolution, electrical properties and thermochemical stability of $BaCo_{0.9-x}Fe_xNb_{0.1}O_{3-\delta}$ ceramic membrane, International Journal of Hydrogen Energy 35 (2010) 814–820.

[7] L.D. Conceicao, A.M. Silva, N.F. Ribeiro, M.M. Souza, Combustion synthesis of $La_{0.7}Sr_{0.3}Co_{0.5}Fe_{0.5}O_3$ (LSCF) porous materials for application as cathode in IT-SOFC, Materials Research Bulletin 46 (2011) 308–314.

[8] M.S. Toprak, M. Darab, G.E. Syvertsen, M. Muhammed, Synthesis of nanostructured BSCF by oxalate co-precipitatione As potential cathode material for solid oxide fuels cells, International Journal of Hydrogen Energy 35 (2010) 9448–9454.

[9] A.P. Khandale, S.S. Bhoga, Electrochemical performance of microwave synthesized $Nd_{1.8}Ce_{0.2}CuO_{4+\delta}$ cathode for intermediate temperature solid oxide fuel cell applications, Journal of Alloys and Compounds 509 (2011) 6955–6961.

[10] A. Hagiwara, N. Hobara, K. Takizawa, K. Sato, H. Abe, M. Naito, Preparation of LSM/ScSZ composite powder materials by spray pyrolysis for the pre-fabrication of SOFC cathodes, Solid State Ionics 178 (2007) 1552–1562.

[11] R. Chiba, F. Yoshimura, Y. Sakurai, Y. Tabata, M. Arakaw, A study of cathode materials for intermediate temperature SOFCs prepared by the sol–gel method, Solid State Ionics 175 (2004) 23–27.

[12] E. Reverchon, R. Adami, Nanomaterials and supercritical fluids, Journal of Supercritical Fluids 37 (2006) 1–22.

[13] A. Tarancon, S.J. Skinner, R.J. Chater, F.H. Ramıreza, J.A. Kilner, Layered perovskites as promising cathodes for intermediate temperature solid oxide fuel cells, Journal of Materials Chemistry 17 (2007) 3175–3181.

[14] K. Zhang, L. Ge, R. Ran, Z.P. Shao, S.M. Liu, Synthesis, characterization and evaluation of cation-ordered $LnBaCo_2O_{5+\delta}$ as materials of oxygen permeation membranes and cathodes of SOFCs, Acta Materialia 56 (2008) 4876–4889.

[15] Y. Lee, D.Y. Kim, G.M. Choi, $GdBaCo_2O_{5+x}$ cathode for anode-supported ceria SOFCs, Solid State Ionics 192 (2011) 527–530.

[16] C. Zhu, X. Liu, C. Yi, D. Yan, W. Su, Electrochemical performance of $PrBaCo_2O_{5+\delta}$ layered perovskite as an intermediate-temperature solid oxide fuel cell cathode, Journal of Power Sources 185 (2008) 193–196.

[17] N. Li, Z. Lu, B. Wei, X. Huang, K. Chen, Y. Zhang, W. Su, Characterization of $GdBaCo_2O_{5+\delta}$ cathode for IT-SOFCs, Journal of Alloys and Compounds 454 (2008) 274–279.

[18] D. Chen, R. Ran, K. Zhang, J. Wang, Z. Shao, Intermediate temperature electrochemical performance of a polycrystalline $PrBaCo_2O_{5+\delta}$ cathode on samarium-doped ceria electrolyte, Journal of Power Sources 188 (2009) 96–105.

[19] A. Chang, S.J. Skinner, J.A. Kilner, Electrical properties of $GdBaCo_2O_{5+x}$ for ITSOFC applications, Solid State Ionics 177 (2006) 2009–2011.

[20] Q. Zhou, T. He, Y. Ji, $SmBaCo_2O_{5+x}$ double-perovskite structure cathode material for intermediate-temperature solid-oxide fuel cells, Journal of Power Sources 185 (2008) 754–758.

[21] H. Gu, H. Chen, L. Gao, Y. Zheng, X. Zhu, L. Guo, Oxygen reduction mechanism of $NdBaCo_2O_{5+\delta}$ cathode for intermediate-temperature solid oxide fuel cells under cathodic polarization, International Journal of Hydrogen Energy 34 (2009) 2416–2420.

[22] Y. Liu, $YBaCo_2O_{5+\delta}$ as a new cathode material for zirconia-based solid oxide fuel cells, Journal of Alloys and Compounds 477 (2009) 860–862.

[23] J.H. Kim, A. Manthiram, $LnBaCo_2O_{5+\delta}$ oxides as cathodes for intermediate-temperature solid oxide fuel cells, Journal of the Electrochemical Society 155 (2008) B385–B390.

[24] S.V. Moharil, B.S. Nagrare, S.P. Shaikh, Nanostructured MIEC $Ba_{0.5}Sr_{0.5}Co_{0.6}Fe_{0.4}O_{3-\delta}$ (BSCF5564) cathode for IT-SOFC by nitric acid aided EDTA–citric acid complexing process (NECC), International Journal of Hydrogen Energy 37 (2012) 5208–5215.

[25] L.D. Conceic, A.M. Silva, N.F. Ribeiro, M.M. Souza, Combustion synthesis of $La_{0.7}Sr_{0.3}Co_{0.5}Fe_{0.5}O_3$ (LSCF) porous materials for application as cathode in IT-SOFC, Materials Research Bulletin 46 (2011) 308–314.

[26] L.D. Conceic, N.F. Ribeiro, J.G. Furtado, M.M. Souza, Effect of propellant on the combustion synthesized Sr-doped $LaMnO_3$ powders, Ceramics International 35 (2009) 1683–1687.

[27] A. Subramania, T. Saradha, S. Muzhumathi, Synthesis of nano-crystalline $(Ba_{0.5}Sr_{0.5})Co_{0.8}Fe_{0.2}O_{3-\delta}$ cathode material by a novel sol–gel thermolysis process for IT-SOFCs, Journal of Power Sources 165 (2007) 728–732.

[28] S. Cardea, A. Gugliuzza, M. Sessa, M.C. Aceto, E. Drioli, E. Reverchon, Supercritical gel drying: a powerful tool for tailoring symmetric porous PVDF-HFP membranes, ACS Applied Materials and Interfaces 35 (2009) 171–180.

[29] W. Zhou, Z. Shao, R. Ran, P. Zeng, H. Gu, W. Jin, N. Xu, $Ba_{0.5}Sr_{0.5}Co_{0.8}Fe_{0.2}O_{3-\delta}+LaCoO_3$ composite cathode for $Sm_{0.2}Ce_{0.8}O_{1.9}$ electrolyte based intermediate-temperature solid-oxide fuel cells, Journal of Power Sources 168 (2007) 330–337.

[30] C. Jin, J. Liu, Y. Zhang, J. Sui, W. Guo, Characterization and electrochemical performances of $Ba_{2-x}Sr_xFeO_{4+\delta}$ as a novel cathode material for intermediate-temperature solid oxide fuel cells, Journal of Power Sources 182 (2008) 482–488.

[31] Y.Q. Guo, Y.M. Yin, Z. Tong, J.W. Yin, M.W. Xiong, Z.F. Ma, Impact of synthesis technique on the structure and electrochemical characteristics of $Pr_{0.6}Sr_{0.4}Co_{0.2}Fe_{0.8}O_{3-\delta}$ (PSCF) cathode material, Solid State Ionics 193 (2011) 18–22.

[32] S.B. Adler, Mechanism and kinetics of oxygen reduction on porous La_{1-x} Sr_x $CoO_{3-\delta}$ electrodes, Solid State Ionics 111 (1998) 125–134.

[33] S.B. Adler, Limitations of charge-transfer models for mixed-conducting oxygen, Solid State Ionics 135 (2000) 603–612.

[34] N. Li, Z. Lu, B. Wei, X. Huang, Y. Zhang, W. Su, Compaction pressure effect on microstructure and electrochemical performance of $GdBaCo_2O_{5+\delta}$ cathode for IT-SOFCs, Ceramics International 38 (2012) 2159–2164.